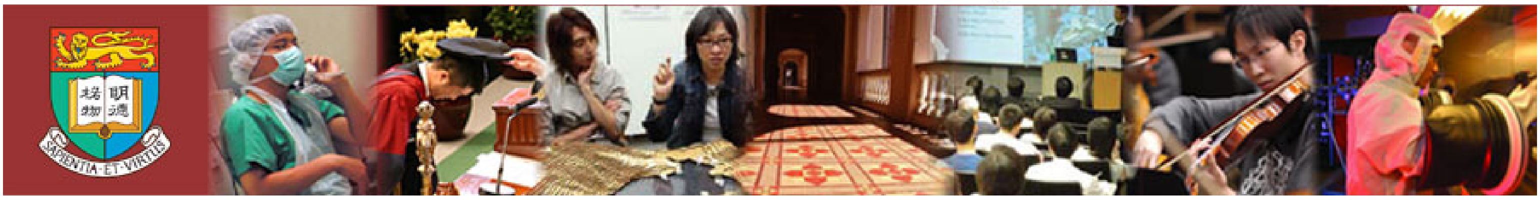

Title	**Improved interfacial and electrical properties of Ge-based metal-oxide-semiconductor capacitor with LaTaON passivation layer**
Author(s)	**Ji, FENG; Xu, J; Huang, Y; Liu, L; Lai, PT**
Citation	**IEEE Transactions on Electron Devices, 2014, v. 61 n. 11, p. 3608-3612**
Issued Date	**2014**
URL	**http://hdl.handle.net/10722/218747**
Rights	**IEEE Trans. Electron Devices. Copyright © IEEE.**

Improved Interfacial and Electrical Properties of Ge-Based Metal-Oxide-Semiconductor Capacitor With LaTaON Passivation Layer

Feng Ji, Jing-Ping Xu, Yong Huang, Lu Liu, and P. T. Lai, *Senior Member, IEEE*

***Abstract*—The interfacial and electrical properties of Ge-based metal–oxide–semiconductor (MOS) capacitor with high-*k* gate dielectric of HfTiO and passivation interlayer of LaTaON are investigated. Experimental results show the Ge MOS with HfTiO/LaTaON gate-stacked dielectric exhibits low interface-state density (7.8 x 10^{11} cm^{-2} eV^{-1}), small gate-leakage current (7.88 x 10^{-4} A cm^{-2} at $V_g - V_{fb} = 1$ V), small capacitance equivalent thickness (1.1 nm), and large equivalent dielectric constant (27.7). X-ray photoelectron spectroscopy and transmission electron microscopy reveal that the improvements should be due to the fact that La/Ta-based oxide/oxynitride has excellent interface properties with Ge, and the LaTaON interlayer can effectively block the in-diffusion of oxygen and the out-diffusion of germanium, thus suppressing the growth of low-*k* GeO_x and intermixing between Ge and Hf.**

***Index Terms*—Ge metal–oxide–semiconductor (Ge MOS), high-*k* dielectric, interface properties, LaTaON, passivation layer.**

I. INTRODUCTION

TO KEEP scaling down the size and increase the operating speed of integrated circuits, Ge-based MOSFET with high-*k* gate dielectric has been widely studied owing to its higher electron and hole mobilities than those of silicon [1], and easier integration of Ge on Si than III–V materials. However, unstable and water-soluble GeO-x ($x < 2$) degrades the interface quality, resulting in poor electrical properties. Although the GeO_2/Ge system shows excellent interface properties [2], it is difficult to obtain pure GeO_2. So, different surface passivation layers such as GeON [3] and AlON [4] have been investigated, which exhibited good interface properties. However, their low *k* values (~9 for AlO_xN_y [5] and 6–7 for GeO_xN_y [6]) block the reduction of the equivalent oxide thickness (EOT) and thus limit the further scaling of MOS device. Amorphous $LaAlO_xN_y$ ($k \sim 30$) has shown excellent interface quality with Si [7], and it is expected that good interface property with Ge could also be obtained. To increase the *k* value, it is necessary to replace Al oxide by other metal oxides with higher *k* value. Ta_2O_5 has a *k* value of 25–26 [8], [9], and TaO_xN_y (which underwent a high-temperature rapid thermal nitridation at ~800 °C without crystallization [8]) has a larger *k* value than Ta_2O_5 [10]. So, both TaO_xN_y and Ta_2O_5 have a higher *k* value than AlO_xN_y and Al_2O_3 (~9) [9]. In addition, La_2O_3 exhibits a high *k* value of ~30 [9], good thermal stability and scalability (EOT can be scaled down to ~0.5 nm) [11]. Therefore, it should be a good choice to substitute Al oxide/oxynitride by Ta oxide/oxynitride to form high-*k* LaTaON dielectric as passivation interlayer with high *k* value and good interface quality. On the other hand, Hf-based oxide with wide band gap (~6 eV), as one of the most promising high-*k* materials, is employed as gate dielectric. Because the electrical properties of the device would be degraded owing to intermixing between Ge and Hf [1]–[12], it is expected that the LaTaON interlayer could play a role of blocking the out-diffusion of Ge, thus isolating Ge and Hf. In addition, to further increase the *k* value of the gate dielectric, Ti oxide with higher *k* value is incorporated in the Hf oxide. Therefore, Ge-based MOS with LaTaON as passivation interlayer and HfTiO as high-*k* gate dielectric is proposed and prepared with a postdeposition annealing (PDA) in dry N_2 ambient in this paper. As a result, excellent electrical and interface properties are obtained for the device.

II. EXPERIMENTS

MOS capacitors were fabricated on N-type (100) Ge wafers with a resistivity of 0.10–0.11 Ω cm. The wafers were cleaned in organic solvent followed by dipping in diluted HF (1:50) for 30 s, and then rinsed in deionized water for several times to remove the native oxide. After drying by N_2, the wafers were transferred immediately to the vacuum chamber of a sputtering system. A ~2 nm LaTaN film was deposited by cosputtering of La and Ta targets at room temperature in an Ar/N_2 (=24/6) ambient, followed by a deposition of ~5 nm HfTiO film by cosputtering of Hf and Ti targets in an Ar/O_2 (=24/3) ambient (denoted as stacked sample). Then, PDA was carried out in N_2 (500 ml/min) + O_2 (50 ml/min) at 500 °C for 300 s

---

Manuscript received June 17, 2014; revised August 26, 2014; accepted September 2, 2014. Date of publication September 19, 2014; date of current version October 20, 2014. This work was supported in part by the National Natural Science Foundation of China under Grant 61274112 and Grant 61176100 and in part by the Hubei Provincial Department of Education Scientific and Technological Research Projects under Grant B2013263. The review of this paper was arranged by Editor N. Bhat.

F. Ji is with Wuhan Polytechnic, Wuhan 430074, China.

J.-P. Xu, Y. Huang, and L. Liu are with the School of Optical and Electronic Information, Huazhong University of Science and Technology, Wuhan 430074, China (e-mail: jpxu@hust.edu.cn).

P. T. Lai is with the Department of Electrical and Electronic Engineering, University of Hong Kong, Hong Kong (e-mail: laip@eee.hku.hk).

Color versions of one or more of the figures in this paper are available online at http://ieeexplore.ieee.org.

Digital Object Identifier 10.1109/TED.2014.2356597

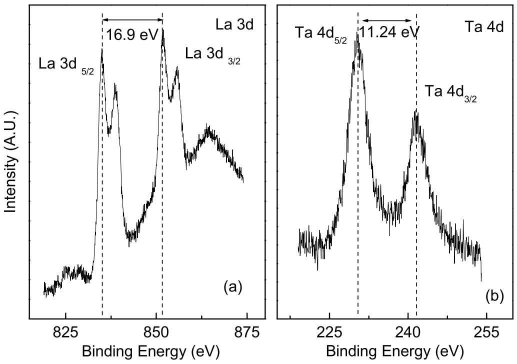

Fig. 1. XPS spectra of LaTaON/Ge system. (a) La 3d. (b) Ta 4d.

to transform LaTaN into LaTaON. For comparison, a MOS capacitor with HfTiO gate dielectric but no LaTaON interlayer was fabricated (denoted as nonstacked sample). Al was e-beam evaporated and patterned using lithography as the gate electrode with an area of 7.85 × 10^{-5} cm^2. Finally, the samples were annealed at 300 °C for 20 min in forming gas ($N_2/H_2 = 95/5$). To investigate the interlayer formation by X-ray photoelectron spectroscopy (XPS), one sample with only thin LaTaON layer (∼2 nm) was fabricated on Ge. In addition, to more clearly observe the LaTaON layer and LaTaON/Ge interface by transmission electron microscopy (TEM), another sample with only slightly thicker LaTaON film (∼5 nm) on Ge wafer was also fabricated. Both samples were prepared under the aforementioned conditions.

High-frequency (1 MHz) C–V curve and gate-leakage current density (J_g) of the samples were measured at room temperature by using HP4284A precision LCR meter and HP4156A precision semiconductor parameter analyzer, respectively. The physical thickness of the gate dielectric (t_{ox}) of the samples was determined by a multiwavelength ellipsometer. XPS was employed to determine the elements of the LaTaON/Ge system while TEM was used to observe the LaTaON/Ge interface. The surface roughness of gate dielectric of both samples was measured by atomic force microscope (AFM). All electrical measurements were carried out under a light-tight and electrically shielded condition.

III. RESULTS AND DISCUSSION

The composition of the LaTaON film was investigated using XPS analysis. The spectrum of La 3d is shown in Fig. 1(a). Two strong peaks at 851.7 eV (La $3d_{3/2}$) and 834.8 eV (La $3d_{5/2}$) are detected. The spin-orbit splitting energy of 16.9 eV is in accordance with the 16.9 eV of La_2O_3/LaON [13], showing the presence of La_2O_3/LaON in the interlayer. Ta $4d_{3/2}$ and Ta $4d_{5/2}$ peaks are also detected and shown in Fig. 1(b). The spin-orbit splitting energy is ∼11.24 eV, thus indicating the presence of Ta^{+5} from Ta_2O_5/TaON [14].

The spectrum of Ta 4f is shown in Fig. 2(a), and two peaks are located at 28.14 eV (Ta $4f_{5/2}$) and 26.24 eV (Ta $4f_{7/2}$). The spin-orbit splitting energy of 1.9 eV corresponds to Ta^{5+}, further indicating the formation of TaON [15], [16] and Ta_2O_5 [15]–[18]. Fig. 3(a) shows the spectrum of O 1s and its peak position is 531 eV, which is closer to 530.9 eV (Ta_2O_5) and 530.8 eV (TaON) [15]. In addition, N 1s is also detected, as shown in Fig. 3(b), indicating that nitrogen is incorporated in the film. These results show that LaTaON layer has been formed.

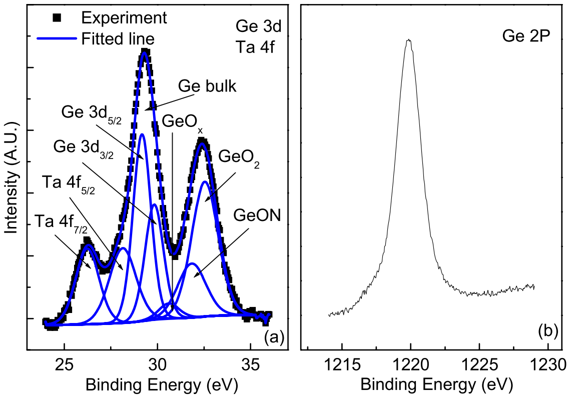

Fig. 2. XPS spectra of LaTaON/Ge system. (a) Ta 4f and Ge 3d. (b) Ge 2p.

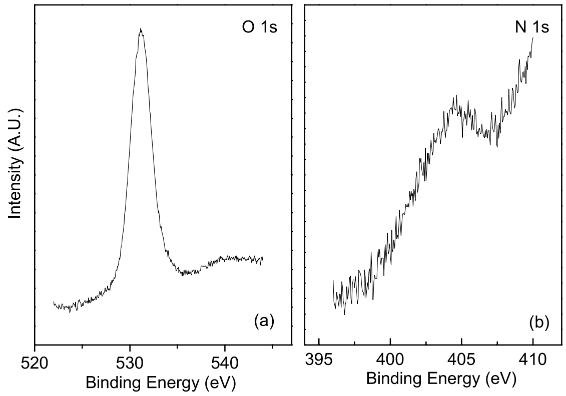

Fig. 3. XPS spectra of LaTaON/Ge system. (a) O 1s. (b) N 1s.

The interface quality of LaTaON/Ge is analyzed by XPS and TEM results. For XPS spectra of Ge as shown in Fig. 2(a), in addition to a doublet of $3d_{5/2}$ and $3d_{3/2}$ from Ge bulk [19], [20], the spectra were deconvoluted into three subpeaks by using an XPS analysis software (Thermo Scientific Avantage). The 32.54 eV subpeak coincides with that of GeO_2 (32.3–33.6 eV) reported in [21]–[25], and the peak splitting of 3.24 eV with Ge bulk is in agreement with that of the formation of GeO_2 (3.2 eV) [26]. The spectrum of Ge 2p is shown in Fig. 2(b). The main peak position at 1219.9 eV is in good agreement with the value of 1220.0 eV [20] and 1220.2–1220.6 eV [27] reported for GeO_2. A subpeak with binding energy shift of 2.54 eV from Ge bulk was shown in Fig. 2(a), which indicates nitrogen incorporation and formation of GeON [28], because nitridation can change the chemical state and result in the subpeak shifted to a lower binding energy. A weak subpeak located at 30.62 eV is detected and the peak splitting (∼1.32 eV) relative to Ge bulk is lowest, showing the existence of GeO_x ($x < 2$) [29]. These results demonstrate that there are GeO_2, GeON, and GeO_x at or near the interface of LaTaON/Ge. In addition, it should be

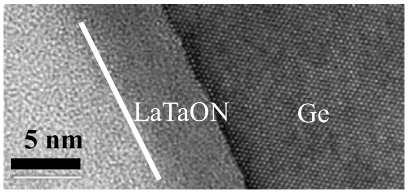

Fig. 4. Cross-sectional HR-TEM image of the LaTaON/Ge system.

noticed that the subpeak of spectrum of GeO_x is far below that of GeO_2 and GeON, and their area ratio is 0.662:0.279:0.057 for GeO_2:GeON:GeO_x, indicating that the content of GeO_x is far less than that of GeO_2 and GeON, that is, the growth of unstable GeO_x is effectively suppressed, while there was an obvious GeO_x layer in HfTiO/Ge MOS according to our previous work [5]. So, the mechanism involved is that the in-diffusion of oxygen and the out-diffusion of germanium are prevented to a large extent owing to the blocking role of the LaTaON interlayer. GeO_2/GeON at or near the interface decreases the equivalent k value of gate dielectric, but unlike GeO_x, GeO_2/GeON would not degrade the interface quality. The good interface quality between the La/Ta-based oxide or oxynitride and Ge is further confirmed by the high-resolution (HR)-TEM image of the LaTaON/Ge system, as shown in Fig. 4. It can be seen that the LaTaON/Ge interface is abrupt and smooth, and there is no obvious interlayer between the LaTaON film and Ge substrate, implying that GeO_2 and GeON detected by XPS are included in the LaTaON interlayer. Using TEM and HR Rutherford backscattering spectrometry, KaMata compared ZrO_2/Ge MOS and HfO_2/Ge MOS [1]. Because ZrO_2 could intermix with GeO_2 in ZrO_2/Ge MOS, there was no interlayer formed, and also no GeO in ZrO_2 was detected. However, for the HfO_2/Ge MOS, because Ge could diffuse into HfO_2 through a reaction between HfO_2 and Ge [1], there was an obvious interlayer (GeO) formed [1]–[12]. For our nonstacked sample, Ge can diffuse into HfTiO through the reaction between HfTiO and Ge to form Ge–O complex (i.e., GeO interlayer), which degrades the interface quality, increases oxide leakage, decreases the equivalent k-value of the gate dielectric, and thus increases EOT. The phenomena in the proposed LaTaON/Ge system are similar to those in the ZrO_2/Ge system. Also, it was reported that there was no reaction between La and Ge [12]. Therefore, it can be concluded that LaTaON can intermix with GeO_2/GeON like ZrO_2, thus suppressing the undesirable formation of GeO_x ($x < 2$). Therefore, LaTaON is a potential dielectric material as the interlayer of Ge MOS to effectively suppress the growth of GeO_x and improve the interface properties.

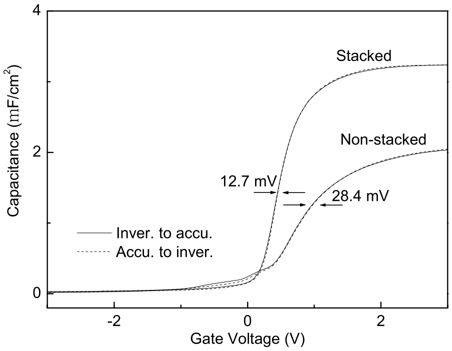

Fig. 5. HF C–V curve of the samples, swept in both directions. Area of capacitor is 7.85×10^{-5} cm^2.

TABLE I

ELECTRICAL AND PHYSICAL PARAMETERS EXTRACTED FROM HF C–V CURVE

Sample	Stacked	Non-stacked
V_{fb} (V)	0.218	0.330
D_{it} ($cm^{-2}eV^{-1}$)	7.8×10^{11}	2.7×10^{12}
Q_{ox} (cm^{-2})	-2.13×10^{12}	-2.76×10^{12}
t_{ox} (nm)	7.6	8.1
CET (nm)	1.1	1.7
k	27.7	18.6

Fig. 5 shows the typical HF C–V curves of the stacked and nonstacked samples. The nonstacked sample has smaller accumulation capacitance, implying the presence of a low-k GeO_x interlayer. However, the stacked sample has a larger accumulation capacitance, which should be due to the suppression of the low-k GeO_x interlayer caused by the blocking role of the LaTaON interlayer against the in-diffusion of oxygen and the out-diffusion of germanium, as mentioned above. As a result, for the nonstacked sample, a stretch out of the C–V curve and small kink in the depletion region are obviously observed, indicating high interface-state density. On the other hand, for the stacked sample, the slope of the C–V curve is larger and no distortion occurs, implying a high-quality LaTaON/Ge interface, which is further supported by a smaller hysteresis of the stacked sample (12.7 mV) than that of the nonstacked sample (28.4 mV).

The flatband voltage (V_{fb}) of the samples is determined from their flatband capacitance [30], and oxide-charge density (Q_{ox}) is calculated as $-C_{ox}(V_{fb} - \phi_{ms})/q$, where ϕ_{ms} is the work-function difference between Al and Ge and C_{ox} is the accumulation capacitance per unit area, as shown in Fig. 5. The interface-state density at or near midgap (D_{it}) is estimated from the 1 MHz C–V curve using the Terman's method [31] for the purpose of comparison, as listed in Table I. Obviously, lower interface-state density is obtained for the stacked sample, indicating a high-quality LaTaON/Ge interface, which is further supported by the small frequency dispersion of the C–V curve for the stacked sample shown in Fig. 6. The capacitance equivalent thickness (CET) is calculated ($CET = k_0 k_{SiO_2}/C_{ox}$, where k_0 and k_{SiO_2} are the permittivity of vacuum and dielectric constant of SiO_2, respectively) and also listed in Table I. Obviously, the stacked sample shows smaller CET than the nonstacked sample, because of the suppressed growth of low-k GeO_x. In addition, the LaTaON interlayer can also hold back the interdiffusions of Ge and Hf, as shown by the clear LaTaON/Ge interface in Fig. 4. So, the stacked sample possesses better interface properties than the nonstacked sample owing to the absence of GeO_x and suppression of the interdiffusion [32]. The smaller Q_{ox} of the stacked sample further indicates the blocking role of the LaTaON interlayer against the interdiffusion of elements. In Table I,

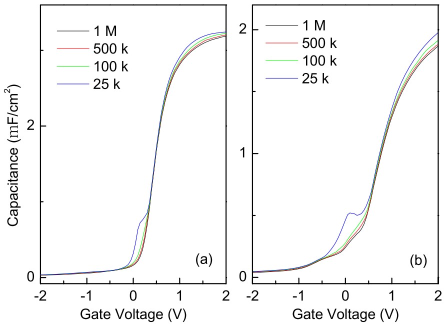

Fig. 6. Frequency dispersion of C–V curve at room temperature. (a) Stacked sample. (b) Nonstacked sample.

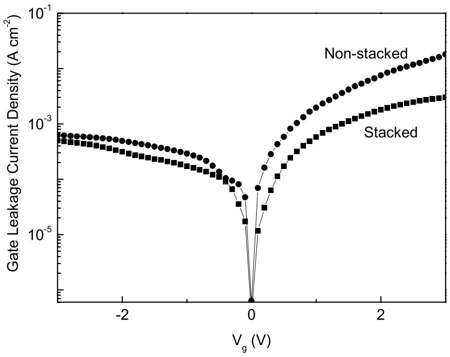

Fig. 7. Typical gate-leakage properties of the samples.

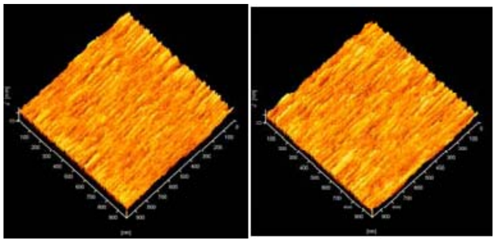

(a) (b)

Fig. 8. AFM image of gate-dielectric surface. (a) Stacked sample. (b) Nonstacked sample.

the equivalent k value of gate dielectric is also calculated by $k = k_{SiO_2} t_{ox}/\mathrm{CET}$. A larger k value (27.7) is obtained for the stacked sample than the nonstacked sample (18.6) owing to the effective suppression of the GeO_x interlayer.

Fig. 7 shows the typical gate-leakage properties of the two samples. The leakage current for 15 devices is in a range of 0.35–0.78 mA cm^{-2} at $V_g = 1$ V and 0.09–0.22 mA cm^{-2} at $V_g = -1$ V for the stacked sample, and 1.37–3.03 mA cm^{-2} at $V_g = 1$ V and 0.17–0.42 mA cm^{-2} at $V_g = -1$ V for the nonstacked sample. Obviously, the stacked sample has lower gate-leakage current than the nonstacked sample, due to the absence of undesirable GeO_x, the suppression of intermixing between Ge and Hf, and the improvements of interface and near-interface properties (small D_{it} and Q_{ox} as listed in Table I). In addition, the AFM image of the gate-dielectric surface of both samples is shown in Fig. 8. The roughness of the stacked sample and nonstacked sample is 0.36 and 0.38 nm, respectively. The smaller surface roughness of the former can also contribute to the reduction of its leakage current [33].

IV. CONCLUSION

In summary, Ge-surface passivation is performed using a LaTaON interlayer to improve the electrical performances of Ge MOS capacitors with high-k HfTiO gate dielectric. Excellent interfacial and electrical properties are obtained, for example, small gate-leakage current, large k value, low interface-state and oxide-charge densities. The involved mechanisms lie in that La/Ta-based oxide or oxynitride have excellent interface properties on Ge, and the LaTaON interlayer can effectively block the in-diffusion of oxygen and the out-diffusion of germanium, thus preventing the intermixing between Ge and Hf, and suppressing the growth of unstable low-k GeO_x.

REFERENCES

[1] Y. Kamata, “High-*k*/Ge MOSFETs for future nanoelectronics,” *Mater. Today*, vol. 11, nos. 1–2, pp. 30–38, Jan./Feb. 2008.

[2] R. Xie, W. He, M. Yu, and C. Zhu, “Effects of fluorine incorporation and forming gas annealing on high-*k* gated germanium metal–oxide–semiconductor with GeO_2 surface passivation,” *Appl. Phys. Lett.*, vol. 93, no. 7, pp. 073504-1–073504-3, Aug. 2008.

[3] C. O. Chui, F. Ito, and K. C. Saraswat, “Scalability and electrical properties of germanium oxynitride MOS dielectrics,” *IEEE Electron Device Lett.*, vol. 25, no. 9, pp. 613–615, Sep. 2004.

[4] F. Gao, S. J. Lee, J. S. Pan, L. J. Tang, and D.-L. Kwong, “Surface passivation using ultrathin AlN_x film for Ge–metal–oxide–semiconductor devices with hafnium oxide gate dielectric,” *Appl. Phys. Lett.*, vol. 86, no. 11, pp. 113501-1–113501-3, Mar. 2005.

[5] C. X. Li and P. T. Lai, “Wide-bandgap high-*k* Y_2O_3 as passivating interlayer for enhancing the electrical properties and high-field reliability of n-Ge metal–oxide–semiconductor capacitors with high-*k* HfTiO gate dielectric,” *Appl. Phys. Lett.*, vol. 95, no. 2, pp. 022910-1–022910-3, Jul. 2009.

[6] K. H. Kim, R. G. Gordon, A. Ritenour, and D. A. Antoniadis, “Atomic layer deposition of insulating nitride interfacial layers for germanium metal oxide semiconductor field effect transistors with high-*k* oxide/tungsten nitride gate stacks,” *Appl. Phys. Lett.*, vol. 90, no. 21, pp. 212104-1–212104-3, May 2007.

[7] X.-B. Lu *et al.*, “Structure and dielectric properties of amorphous $LaAlO_3$ and $LaAlO_xN_y$ films as alternative gate dielectric materials,” *J. Appl. Phys.*, vol. 94, no. 2, pp. 1229–1234, Jul. 2003.

[8] J. Lin, N. Masaaki, A. Tsukune, and M. Yamada, “Ta_2O_5 thin films with exceptionally high dielectric constant,” *Appl. Phys. Lett.*, vol. 74, no. 16, pp. 2370–2372, Apr. 2005.

[9] G. D. Wilk, R. M. Wallace, and J. M. Anthony, “High-*k* gate dielectrics: Current status and materials properties considerations,” *J. Appl. Phys.*, vol. 89, no. 10, pp. 5243–5275, May 2001.

[10] H. Jung, K. Im, H. Hwang, and D. Yang, “Electrical characteristics of an ultrathin (1.6 nm) TaO_xN_y gate dielectric,” *Appl. Phys. Lett.*, vol. 76, no. 24, pp. 3630–3631, Jun. 2000.

[11] Y. H. Wu, M. Y. Yang, A. Chin, W. J. Chen, and C. M. Kwei, “Electrical characteristics of high quality La_2O_3 gate dielectric with equivalent oxide thickness of 5 Å,” *IEEE Electron Device Lett.*, vol. 21, no. 7, pp. 341–343, Jul. 2000.

[12] M. Houssa, G. Pourtois, M. Caymax, M. Meuris, and M. M. Heyns, “First-principles study of the structural and electronic properties of (100)Ge/Ge(M)O_2 interfaces (M=Al, La, or Hf),” *Appl. Phys. Lett.*, vol. 92, no. 24, pp. 242101-1–242101-3, Jun. 2008.

[13] X. D. Huang, J. K. O. Sin, and P. T. Lai, “Nitrided La_2O_3 as charge-trapping layer for nonvolatile memory applications,” *IEEE Trans. Device Mater. Rel.*, vol. 12, no. 2, pp. 306–310, Jun. 2012.

[14] H. Hagiwara, M. Nagatomo, C. Seto, S. Ida, and T. Ishiahara, “Dye modification effects on TaON for photocatalytic hydrogen production from water,” *Catalysts*, vol. 3, no. 3, pp. 614–624, Jul. 2013.

[15] W.-J. Chun *et al.*, "Conduction and valence band positions of Ta_2O_5, TaON, and Ta_3N_5 by UPS and electrochemical methods," *J. Phys. Chem. B*, vol. 107, no. 8, pp. 1798–1803, Feb. 2003.

[16] Q. Gao, S. Wang, Y. Ma, Y. Tang, C. Giordano, and M. Antonietti, "SiO_2-surface-assisted controllable synthesis of TaON and Ta_3N_5 nanoparticles for alkene epoxidation," *Angew. Chem. Int. Ed.*, vol. 51, no. 4, pp. 961–965, Jan. 2012.

[17] M. C. Sekhar, S. Uthanna, R. Martins, S. V. J. Chandra, and E. Elangovan, "The effect of substrate temperature on physical and electrical properties of DC magnetron sputtered $(Ta_2O_5)0.85(TiO_2)0.15$ films," *IOP Conf. Ser., Mater. Sci. Eng.*, vol. 34, no. 1, pp. 012009-1–012009-7, Jan. 2012.

[18] E. Atanassova and D. Spassov, "X-ray photoelectron spectroscopy of thermal thin Ta_2O_5 films on Si," *Appl. Surf. Sci.*, vol. 135, nos. 1–4, pp. 71–82, Sep. 1998.

[19] Q. Xie *et al.*, "TiO_2/HfO_2 Bi-layer gate stacks grown by atomic layer deposition for germanium-based metal–oxide–semiconductor devices using GeO_xN_y passivation layer," *Electrochem. Solid-State Lett.*, vol. 14, no. 5, pp. G27–G30, Mar. 2011.

[20] S. Mallik *et al.*, "$HfAlO_x$ high-*k* gate dielectric on SiGe: Interfacial reaction, energy-band alignment, and charge trapping properties," *Microelectron. Eng.*, vol. 87, no. 11, pp. 2234–2240, Nov. 2010.

[21] A. Užupis, J. Tyczkowski, K. Gubiec, S. Tamulevičius, M. Andrulevičius, and M. Pucėta, "Properties of GexOy:H thin films produced by plasma-assisted chemical vapor deposition," *Mater. Sci.*, vol. 15, no. 1, pp. 7–10, Jan. 2009.

[22] A. Molle, M. N. K. Bhuiyan, G. Tallarida, and M. Fanciulli, "*In situ* chemical and structural investigations of the oxidation of Ge(001) substrates by atomic oxygen," *Appl. Phys. Lett.*, vol. 89, no. 8, pp. 083504-1–083504-3, Aug. 2006.

[23] T. S. Ko, J. Shieh, M. C. Yang, T. C. Lu, H. C. Kuo, and S. C. Wang, "Phase transformation and optical characteristics of porous germanium thin film," *Thin Solid Films*, vol. 516, no. 10, pp. 2934–2938, Mar. 2008.

[24] M. Perego, G. Scarel, M. Fanciulli, I. L. Fedushkin, and A. A. Skatova, "Fabrication of GeO_2 layers using a divalent Ge precursor," *Appl. Phys. Lett.*, vol. 90, no. 16, pp. 162115-1–162115-3, Apr. 2007.

[25] S. Rivillon, Y. J. Chabal, F. Amy, and A. Kahn, "Hydrogen passivation of germanium (100) surface using wet chemical preparation," *Appl. Phys. Lett.*, vol. 87, no. 25, pp. 253101-1–253101-3, Dec. 2005.

[26] A. C. Simonsen, M. Schleberger, S. Tougaard, J. L. Hansen, and A. N. Larsen, "Nanostructure of Ge deposited on Si(001): A study by XPS peak shape analysis and AFM," *Thin Solid Films*, vol. 338, nos. 1–2, pp. 165–171, Jan. 1999.

[27] A. V. Naumkin, A. Kraut-Vass, S. W. Gaarenstroom, and C. J. Powell, "NIST X-ray photoelectron spectroscopy database," in *NIST Standard Reference Database 20, Version 4.1*. Gaithersburg, MD, USA: NIST, 2012.

[28] P. Bhatt, K. Chaudhuri, S. Kothari, A. Nainani, and S. Lodha, "Germanium oxynitride gate interlayer dielectric formed on Ge(100) using decoupled plasma nitridation," *Appl. Phys. Lett.*, vol. 103, no. 17, pp. 172107-1–172107-5, Oct. 2013.

[29] Q. Xie *et al.*, "Germanium surface passivation and atomic layer deposition of high-*k* dielectrics—A tutorial review on Ge-based MOS capacitors," *Semicond. Sci. Technol.*, vol. 27, no. 7, pp. 074012-1–074012-14, Jul. 2012.

[30] J. P. Xu, P. T. Lai, C. X. Li, X. Zou, and C. L. Chan, "Improved electrical properties of germanium MOS capacitors with gate dielectric grown in wet-NO ambient," *IEEE Electron Device Lett.*, vol. 27, no. 6, pp. 439–441, Jun. 2006.

[31] L. M. Terman, "An investigation of surface states at a silicon/silicon oxide interface employing metal–oxide–silicon diodes," *Solid-State Electron.*, vol. 5, no. 5, pp. 285–299, Sep./Oct. 1962.

[32] L. K. Chu *et al.*, "Metal–oxide–semiconductor devices with molecular beam epitaxy-grown Y_2O_3 on Ge," *J. Crystal Growth*, vol. 311, no. 7, pp. 2195–2198, Mar. 2009.

[33] L. Mao, C. Tan, and M. Xu, "Numerical analysis for root-mean-square roughness of SiO_2/Si interface on direct tunneling current in ultrathin MOSFETs," *Solid-State Electron.*, vol. 45, no. 3, pp. 531–534, Mar. 2001.

Feng Ji is currently an Associate Professor with the College of Electronic Information Engineering, Wuhan Polytechnic, Wuhan, China. His current research interests include high-*k* gate dielectric Si- and Ge-MOS devices, and modeling and simulation of small-scaled MOS devices.

Jing-Ping Xu is currently a Professor with the School of Optical and Electronic Information, Huazhong University of Science and Technology, Wuhan, China. His current research interests include high-*k* gate dielectric Si-, Ge-, SiC-, GaAs-, and InGaAs-based MOS devices, modeling and simulation of small-scaled MOS devices, and charge-trapping nonvolatile semiconductor memory.

Yong Huang received the B.S. degree from Hubei Minzu University, Enshi, China, in 2001, and the M.E. degree from Chongqing University, Chongqing, China, in 2008. He is currently pursuing the Ph.D. degree with the Huazhong University of Science and Technology, Wuhan, China.

His current research interests include small-scaled GeOI MOSFETs with high-*k* gate dielectrics.

Lu Liu is currently a Lecturer with the School of Optical and Electronic Information, Huazhong University of Science and Technology, Wuhan, China. Her current research intersts include advanced SONOS nonvolatile memory with high-*k* gate stack and III–V MOSFETs with high-*k* gate dielectrics.

P. T. Lai (M'90–SM'04) is currently a Professor with the Department of Electrical and Electronic Engineering, University of Hong Kong, Hong Kong. His current research interests include thin-gate dielectrics for FET devices based on Si, SiC, GaN, Ge, and organics, and microsensors for detecting gases, heat, light, and flow.